SURFACE ROUGHNESS AND CORRELATED ENHANCED FIELD EMISSION INVESTIGATIONS OF ELECTROPOLISHED NIOBIUM SAMPLES*

A. Navitski#, S. Lagotzky, G. Müller, FB C Physik, Universität Wuppertal, Germany

D. Reschke, X. Singer, DESY, Hamburg, Germany

Abstract

Systematic measurements of the surface roughness and local defects on high purity Nb samples by means of optical profilometry and combined AFM are reported. Flat polycrystalline samples were electropolished inside Nb cavities for surface quality control. Curved samples were cut from interesting surface areas of a nine-cell Nb structure which was limited by low quench fields. The maximum electric field enhancement factor of various types of defects were derived from their measured height and sharpness. Particles and scratches were identified as potentially stronger field emitters than grain boundaries and round hills and holes. Many large pits with crater-like centers and sharp rims were found especially on lower half-cell samples of the electropolished Nb cavity.

INTRODUCTION

Enhanced field emission (EFE) from particulate contaminations or surface irregularities is one of the main field limitations of the high gradient superconducting niobium cavities required for XFEL and ILC [1]. While the number density and size of particulates on metal surfaces can be much reduced by high pressure water rinsing (HPR) [2], dry ice cleaning (DIC) [3] and clean room assembly of the accelerator modules, the influence of surface defects of the actually electropolished and electron-beam-welded Nb surfaces on EFE has been less studied yet.

Here, we report on results of systematic measurements of the average and local surface roughness of typically prepared Nb samples some of which were cut out of a nine-cell polycrystalline Nb cavity. By means of optical profilometry combined with atomic force microscopy (AFM), large scanning ranges as well as high resolution zooms into the found defect areas was obtained. Optical profilometry is considered to be a fast tool for the quality control of the final surface preparation of Nb accelerating structures. Numbers for the average surface roughness and maximum step height of grain boundaries will be given with respect to magnetic field enhancement which might cause high-field Q-drop and quenches [4]. Electric field enhancement factors will be derived from the height and sharpness of the localized defects. After HPR of selected Nb samples at DESY, correlated field emission scanning microscopy (FESM) and high resolution SEM investigations are planned in order to reveal the influence of the defect geometry on the expected EFE.

* Work supported by HGF, Hamburg

navitski@physik.uni-wuppertal.de

EXPERIMENTAL TECHNIQUES

For the measurement of the surface roughness and the localization and characterization of defects we have used a commercial apparatus (FRT GmbH) shown in Fig. 1 [5]. It is mounted on massive granite supports with an active vibration damping system in front of a laminar air flow system (class 5 ISO) for cleanroom-like conditions. The measurement system combines a small CCD camera for fast orientation with an optical profilometer based on a spectral reflection (chromatic aberration) of white light and an AFM in calibrated positions (1 µm precision). Surface profiles of flat as well as curved samples up to 20×20 cm^2 size and 5 cm height difference are measured fast (100×100 pixels in about 1 minute) and non-destructively down to 2 µm lateral and 3 nm vertical resolution. Further zooms into localized defect areas down to 3 nm lateral resolution are performed with the AFM with 34x34 μm^2 scanning range.

Figure 1: FRT optical profilometer combined with AFM.

We have tested six flat and five curved Nb samples. The flat ones with Ø 26.5 mm were machined from usual high-purity Nb sheets (RRR > 300) and welded to support rods which hold them in the main coupler port of nine-cell cavities for the quality control of chemical treatments

[6]. Special marks on the circumference have been made to reidentify their angular position in FESM and SEM setups. The curved samples were cut out of a nine-cell cavity, which suffered from strong quenching at moderate accelerating field of 16 MV/m. These samples were taken from different interesting surface areas: two (one) from the flat part of lower (upper) half cell and one each from the iris and equator weld regions. All samples have obtained comparable electropolishing up to 144 µm, buffered chemical etching up to 10 µm and HPR but were not kept in clean conditions. For the surface roughness and defect measurements reported here, flat samples have been cleaned in ultrasonic isopropyl alcohol bath and dried with an ionizing gun using pressurized filtered nitrogen (5.0).

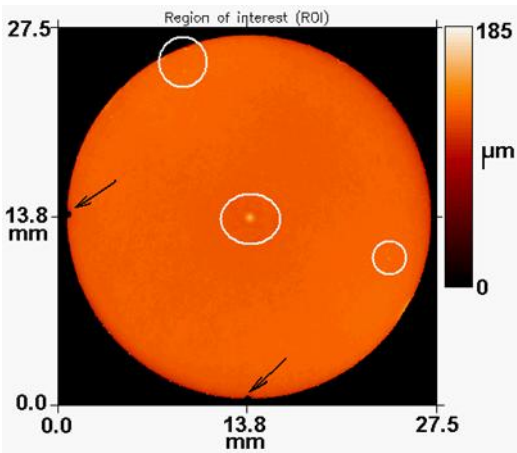

Figure 2: Full profile of a flat Nb sample (30 µm lateral resolution) showing the positions of two marks (arrows) and some big defects on the surface (circles).

The optical profilometer measurements of flat samples have been performed in three steps. At first full scans of the sample (27.5×27.5 mm^2) with a lateral resolution of at least 30 µm were made to localize the major defects with respect to the marks at the circumference as shown in Fig. 2. Then selected regions of typically 5×5 mm^2 size with large defects, which were also obvious by distorted light reflection, were further investigated with at least 10 µm resolution. Finally, interesting defect areas were scanned with maximum resolution of 2 µm over 0.5×0.5 mm^2. It is noteworthy that the full scans of the curved samples were made in several consecutive layers because of the limited height range of the optical profilometer (230 µm). An example for the resulting synthesized 3D view of the equator weld region is presented in Fig. 3. Because of the limited lateral resolution of the optical profilometer, the sharpest features of some localized surface defects were measured with the AFM.

Based on the optical profilometer measurements the average and quadratic surface roughness have been calculated as

$$R_a = \frac{1}{n \cdot m} \sum_{i=1}^{n} \sum_{j=1}^{m} \left| z(x_i y_j) - \bar{z} \right|$$

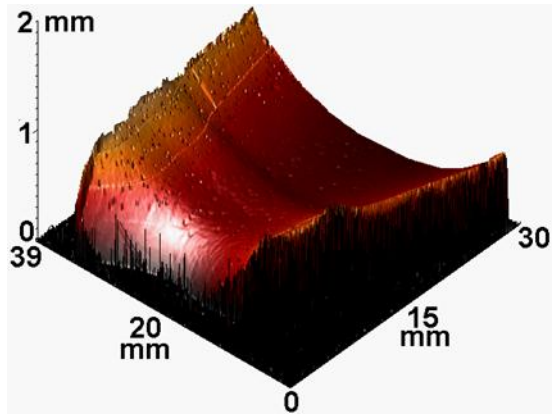

Figure 3: 3D view of a Nb sample cut from the equator region (30 µm lateral resolution) measured in 4 layers showing pits on the surface and the weld seam.

$$R_q = \sqrt{\frac{1}{n \cdot m} \sum_{i=1}^{n} \sum_{j=1}^{m} \left(z(x_i y_j) - \bar{z} \right)^2}$$

where $z(x_i y_j)$ is the actual and $\bar{z}$ the average value of the profile height and n and m are the number of points in x and y directions. For curved surfaces these roughness values can also be determined with respect to the nominal surface shape.

In order to estimate the local electric field enhancement factor β of the defects which might lead to EFE at applied surface fields E_s much below the intrinsic limit given by the Fowler-Nordheim theory (> 1 GV/m for Nb) [7], expected β values of surface defects with height h and tip curvature radius r were roughly calculated by

$$\beta \approx \frac{h}{r} \quad .$$

RESULTS AND DISCUSSION

One of the most remarkable features found especially on electropolished Nb nine-cell cavities are visible pits which appear more densely distributed on the lower than on the upper half cell of vertically treated cavities. We have found such pits on all five curved Nb samples (e.g. in Fig. 3) but less on the weld seams. The detailed optical profiles shown in Fig. 4 reveal their size up to 800 µm in diameter and crater-like centers (~ Ø 200 µm) with sharp rims of 5-10 µm height which might lead to quenches or EFE. Estimation of field enhancement factor leads to β_{max} values of about 9.6 for the rims. The origin of the pits and craters is not clarified yet but we consider them as an etching effect due to the finite time required for washing off the acid solution after electropolishing.

We have also compared the surface roughness of the curved Nb samples in the half-cell and weld regions. The typical profiles given in Fig. 5 show the surprising result that the weld seams are smoother (R_a = 0.115 µm, R_q= 0.159 µm) than the other regions (R_a = 0.180 µm, R_q= 0.250 µm) probably due to the enlarged grain size (640 µm vs. 152 µm). The grain boundaries provide, however,

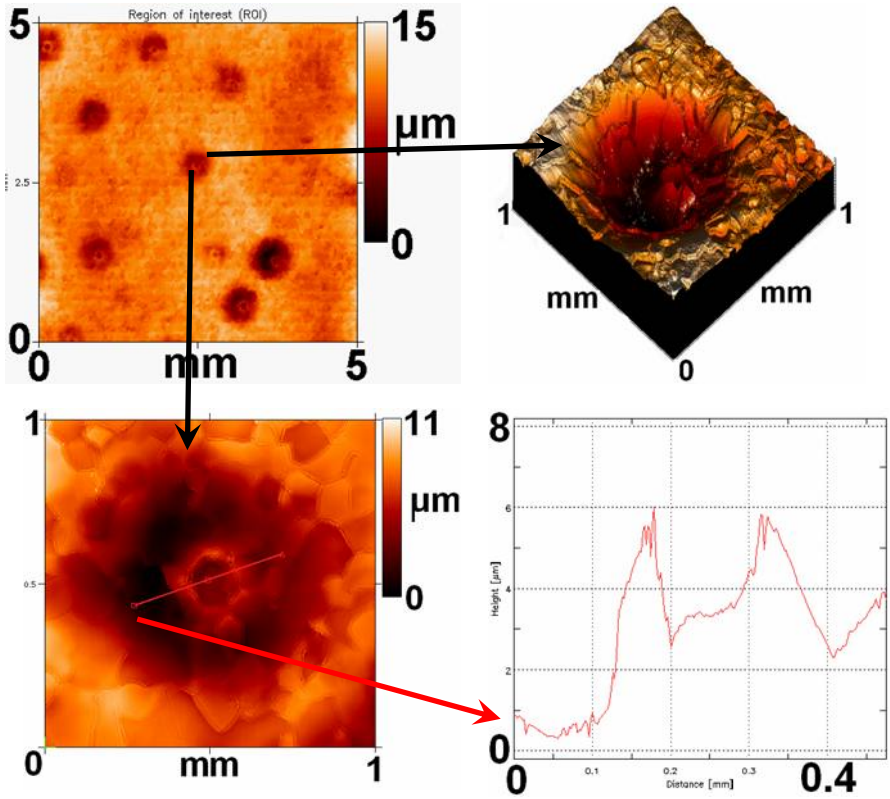

Figure 4: Optical profiles of an upper half-cell part of a tested Nb cavity showing many pits with crater-like elevations and sharp rims in the center. Please note the much enhanced height scale in the 3D view and line profile of the pit.

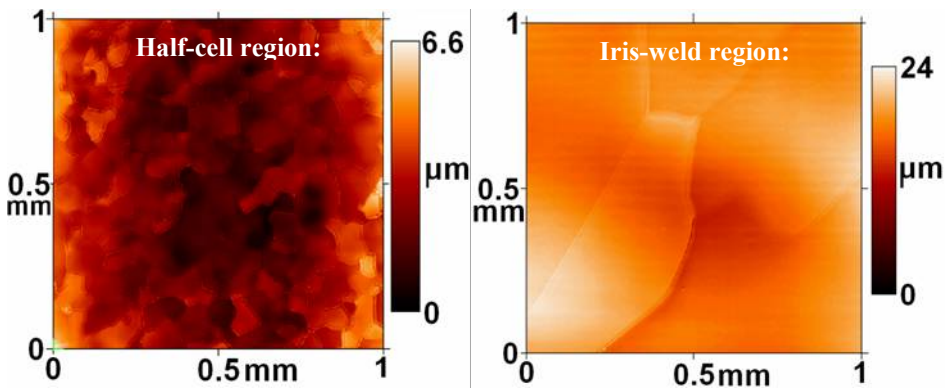

Figure 5: Comparison of high resolution optical profiles of a half-cell and an iris weld region of a tested Nb cavity.

quite similar step height (< 2 µm) and edge radius (< 0.5 µm) resulting in β_{max} ~ 4-5 which should be negligible for EFE.

The optical profiles of the flat Nb samples have shown mainly four types of surface defects: particles (rather than foreign material inclusions), scratch-like protrusions, grain boundaries and round hills and holes (see Figs. 6-7). The geometrical parameters of these defect categories are summarized in Table 1. It is remarkable that the highest β_{max} values were obtained for particles (< 15) and scratch-like protrusions (< 13). Particles have been found on the surfaces more often than scratches. In some cases one could find up to 55 particles in an area of 500×500 µm^2 (Fig. 6a), but surely most of them could be removed by HPR and/or DIC. In contrast, scratches with high and sharp ridges formed by some material shift from the electropolished surface must be avoided during the handling of cavities. (Figs. 6b, d).

Other irregularities found on the flat Nb surfaces are hill-like structures (Fig. 6c) and round holes which are most probably caused by foreign material inclusions which might lead to reduced or enhanced electrochemical polishing, respectively. According to their comparably smooth edges and low β_{max} values (< 4), holes and hill-like structures are not considered as sources of EFE as long as they do not have sharp edges.

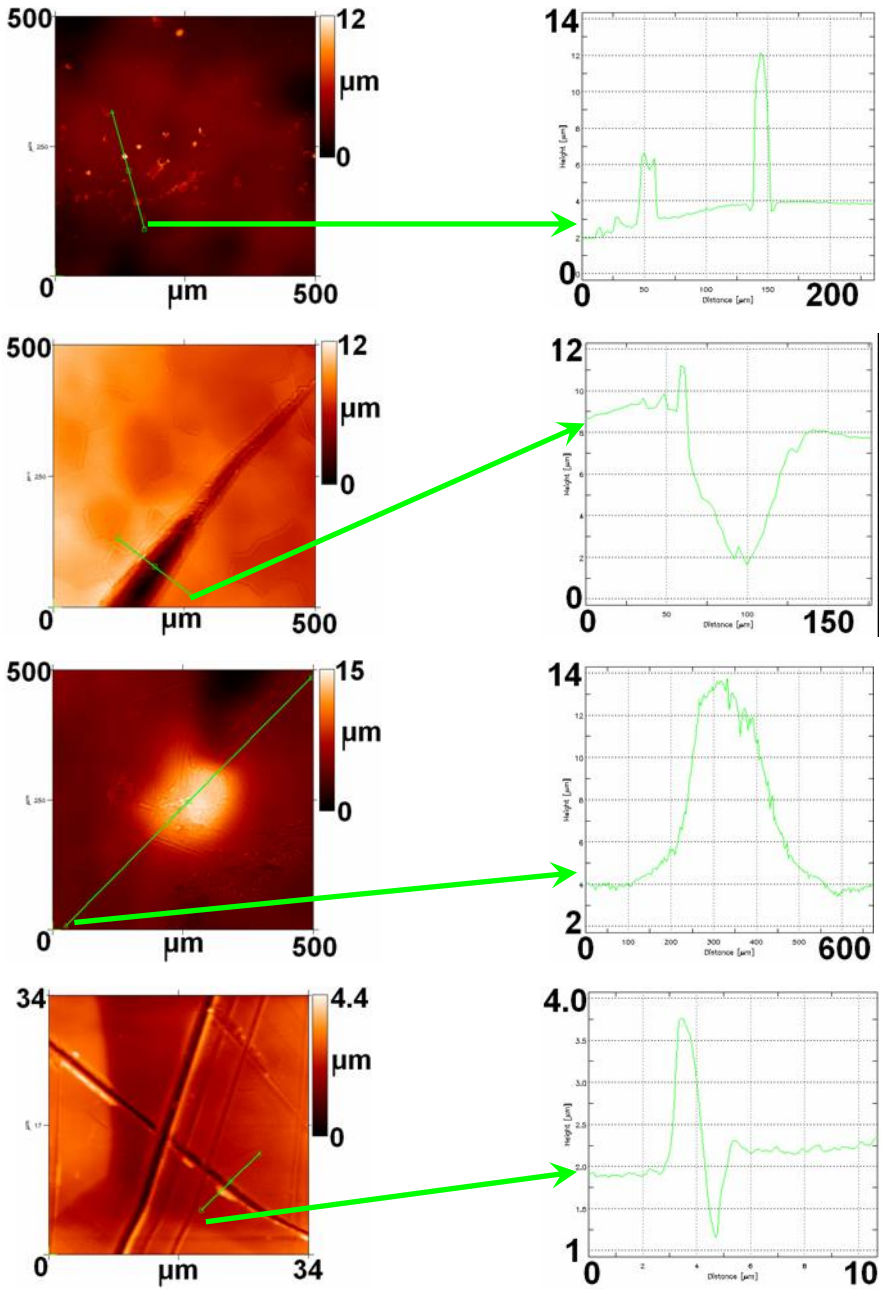

Figure 6: Optical profiles of typical defects found on the flat Nb samples: particles (a), scratches (b), round hills and holes (c) and AFM image of a scratch (d), all with corresponding line profiles.

Table 1: Geometrical Parameters of Defects

Particles		Scratches	Grain boundaries	Round hills and holes
< 5 µm	43 %	4 -100 µm width 11 µm – 2.7 mm length (on average 326 µm) ridge height < 10 µm	step height < 1.55 µm edge radius < 0.78 µm	height < 17 µm size ~ 10 µm - 440 µm
5 - 15 µm	48.4 %			
15 - 25 µm	6.1 %			
> 25 µm	2.5 %			
R_a = 0.276 µm, R_q = 0.548 µm, $\beta_{max} \approx 14.6$		R_a = 0.466 µm, R_q = 0.646 µm, $\beta_{max} \approx 12.9$	$\beta_{max} \approx 4$	R_a = 0.295 µm, R_q = 0.489 µm, $\beta_{max} < 4$

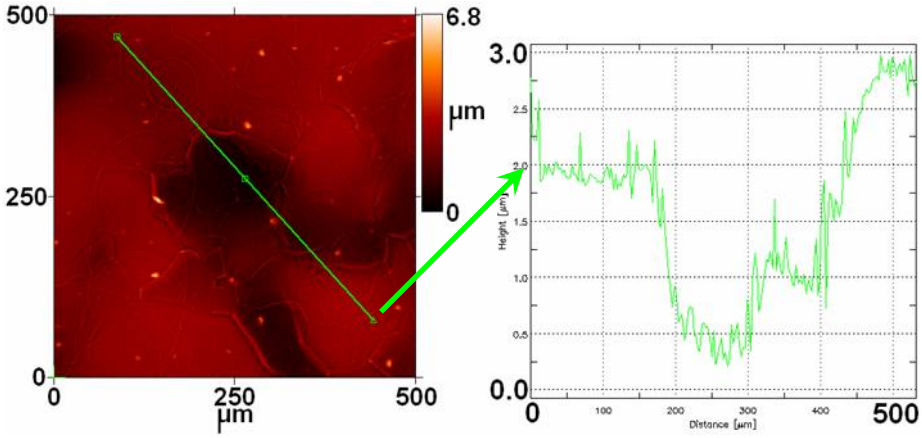

Figure 7: Optical profile and line scan of a flat Nb sample with grain boundary steps.

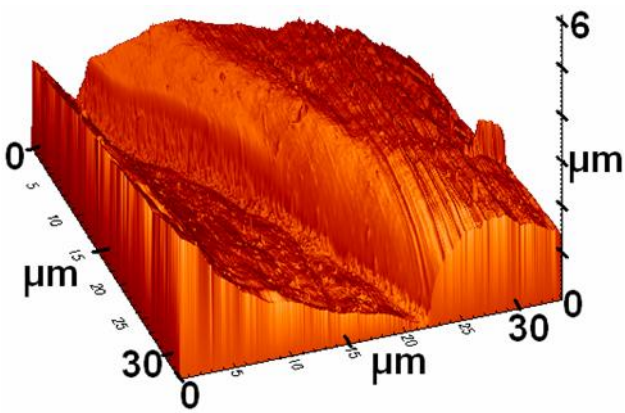

Figure 8: AFM result showing a grain boundary step.

The grain structure of the flat Nb samples shown in Fig. 7 was very similar to that of the curved half-cell ones. The average grain size of about 140 µm and a maximum step height up to 1.55 µm was determined from the optical profiles. AFM zoom scans into selected grain boundaries resulted in more precise measurements of the step edge radius (< 0.78 µm) as shown in Fig. 8. Accordingly, the grain boundaries on the flat Nb samples also provided only low β_{max} values (< 4) which should not cause EFE in high gradient superconducting cavities.

CONCLUSION AND OUTLOOK

Combination of optical profilometry and AFM is suitable as fast quality control of electropolished Nb surfaces in terms of roughness and defects. Remaining particles with $\beta_{max} < 15$ have to be removed by HPR and DIC. Scratch-like protrusions with $\beta_{max} < 13$ must be prevented by a more careful handling. Grain boundaries with step heights < 1.55 µm might reduce the magnetic field limit. Round hills and holes with smooth edges cause less EFE but can be a probable source of quenches. Pits with crater-like centers and sharp rims have been found on real cavity surfaces and hint for problems with the speed of acid removal after the electropolishing.

Correlated field emission scanning microscopy will be performed after HPR (and DIC) of these samples especially in the localized surface defect regions.

ACKNOWLEDGEMENTS

We thank A. Matheisen from DESY for the flat Nb samples. Financial support from the Helmholtz Alliance "Physics at the Terascale" is gratefully acknowledged.

REFERENCES

[1] A. Dangwal et al., Phys. Rev. ST Accel. Beams 12, 023501 (2009).
[2] P. Kneisel and B. Lewis, Proc. of 7th Workshop on RF Superconductivity, Gif sur Yvette (1995), p.311.
[3] A. Dangwal et al., J. Appl. Phys. 102, 044903 (2007).
[4] J. Knobloch et al., Proc. of 9th Workshop on RF Superconductivity, Santa Fe (1999), p.77.
[5] www.frt-gmbh.com
[6] G. Müller et al., Proc. of 6th Eur. Part. Acc. Conf. EPAC 98, Stockholm, p. 1876 (1998).
[7] H. Fowler, L.W. Nordheim, Proc. Royal Soc. (London) A119, 173 (1928).